

# Protrusion Location Optimization in Communication via Diffusion

Goshgar Ismayilov  
Bogazici University  
Istanbul, Turkey  
goshgar.ismayilov@boun.edu.tr

**Abstract**—Molecular communication via diffusion is the state-of-the-art communication paradigm in which information is transmitted between nanomachines through molecules. It enables individual nanomachines to expand their collaborative operability in several applications. The success of molecular communication is greatly hindered by the degradation in the receiver reception performance over the channel. Although the receiver can be reinforced with the protrusions, they have still design issues to be resolved in order to improve the performance further. In this paper, we (1) propose the protrusion location optimization problem by modelling the protrusions as individual features, (2) present ten different algorithms to optimize their locations on the receiver surface and (3) measure the performance of the algorithms with probability of hit metric in two different settings. The experimental results show that Gaussian-distributed protrusions (*GP*) is superior in shorter channels while uniformly-distributed protrusions (*UP*) is superior in longer channels.

## I. INTRODUCTION

*Nanonetworking* is an emergent communication paradigm which involves with information transmission between nanomachines [1], [2]. It extends the capabilities of individual nanomachines in their workspaces to a great extent by enabling information sharing. Nanonetworking opens up major developments and innovative solutions in various applications including accurate drug delivery, genetic material modification and air pollution control [3], [4]. A special type of nanonetworking is molecular communication which interconnects multiple nanomachines altogether to perform complex tasks [5]. The communication among nano-machines is provided with the messenger molecules and diffusion dynamics.

*Molecular communication (MC)* encompasses different techniques as molecular motors [6] for short ranges, communication via diffusion [7] and ion signalling [8] for short to medium ranges and pheromone signalling [9] for long ranges. Specifically, *molecular communication via diffusion (CvD)* comes up from the requirements of efficient communication among nanomachines [10]–[12]. It is consisted of five concurrent operations in general: encoding, emission, propagation, absorption and decoding [13]. The first operation is encoding where the information is reversibly encoded in lossless manner with respect to the modulation technique selected. The reliable encoding is especially important in CvD where trajectories of messenger molecules are unpredictable and they are open to dissipation before reaching to the destination. After the emission of molecules from the transmitter, they independently

travel through the fluid until their absorption. The information is decoded with respect to the demodulation technique [14].

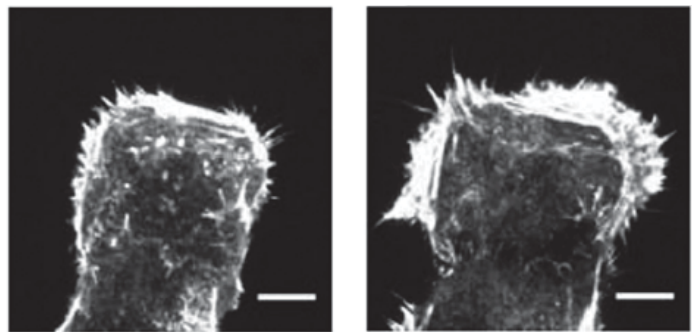


Fig. 1. The total internal reflection fluorescence (TIRF) microscopy image of the protrusions before ( $-60sec$ ) and after ( $500sec$ ) the stimulus addition into the environment [16]

The cellular protrusions are arm-like cytoplasmic extensions from the cell membrane. They are spatially and temporally dynamic structures that involve with vital cell activities in nature. In our work, we use filopodia-like protrusions made of bundling of F-actin filaments [15]. They can extend up to  $10 \mu m$  in length with nano-scale radius. It is biologically shown that the protrusions respond to various stimulus in the environment for migration, invasion and nourishment [16], (see Fig. 1). In our work, the stimulus is considered as varying concentrations of soluble molecules, which leads the protrusions to head towards the source that they are emitted. The adaptation of the protrusions from biology to molecular communication is provided in the work [17] where their locations are randomly chosen.

The location analysis has been confronted in various applications including agricultural activities, public facility allocation and sensor management in the literature [18]–[20]. One of most famous and earliest is known as Fermat-Weber problem, which was proposed in 17th century as follows: "Given three points in a plane, find a location such that the sum of its distances to the three given points is as small as possible" [21]. With that inspiration, we will perform location analysis for the protrusions in our work so that probability of hit of molecules is maximized. It is incontrovertible that although the protrusions are one of key factors to improve the channel performance, the lack of control on their locations could be a major drawback in certain cases. To the best of our

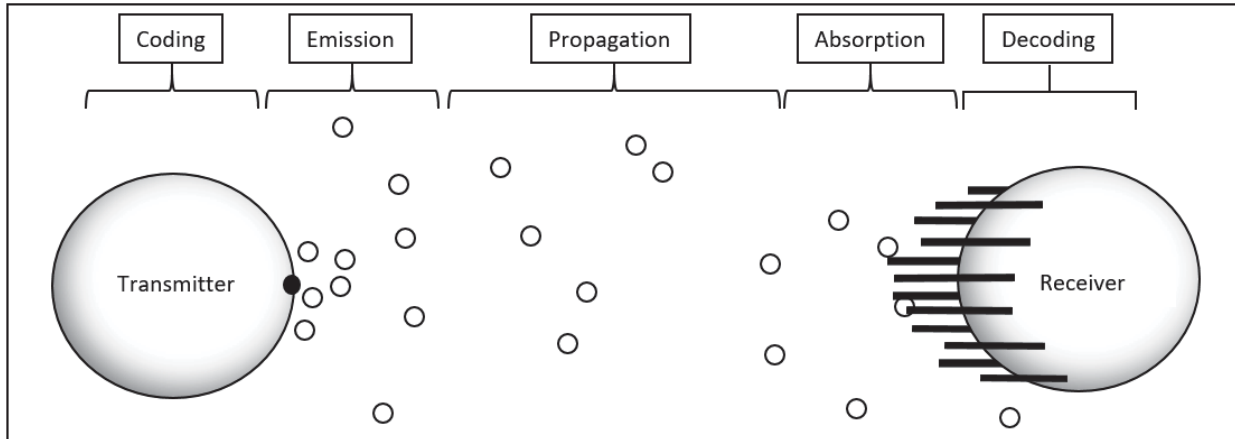


Fig. 2. Communication via Diffusion (CvD) model with the receiver-side protrusions

knowledge, there is no work in the literature to address the location analysis for the protrusions.

The main contributions of the paper can be summarized as follows:

- We propose the protrusion location optimization problem for the maximization of the probability of hit with the minimization of the *inter-symbol interference (ISI)*.
- We present ten different algorithms under four different categories: (1) no protrusion methods, (2) distribution-based methods, (3) heatmap-based methods and finally (4) sequential feature selection methods.
- We perform empirical study to compare the performance of the algorithms under varying channel length and varying number of protrusions.

The rest of the paper is organized as follows. Section 2 describes the system model including communication via diffusion (CvD) and protrusions. Section 3 defines the protrusion location optimization problem and presents ten different algorithms. While Section 4 provides the experimental results, Section 5 concludes the paper.

## II. SYSTEM MODEL

### A. Communication via Diffusion (CvD) Model

The diffusion-based molecular communication is the iterative and probabilistic propagation of messenger molecules inside of a fluid based on Brownian motion. The molecules randomly drifting through the fluid enable the cooperative abilities between nanonetworking-enabled transmitter and receiver by carrying information as carriers. The single transmitter spreads molecules to the fluid from the single release point, which is directed towards the receiver. At the same time, the single receiver tries to capture those molecules with the help of receptors on its surface in the peer-to-peer network. The chemical reactions triggered by receptor-molecule bondings finalize the reception operation. (see Fig. 2)

The information is defined as sequence of symbols in molecular communication. The symbol sent by the transmitter is called as *intended symbol* while the symbol received by the

receiver is called as *received symbol*. The mutual reconciliation of those bodies on symbols are one of the primary purpose of the communication. Therefore, the information sharing between bodies can be provided by different channel modulation techniques. Although there exist many modulations in the literature, their investigations are out of topic for us. In this work, we follow Binary Concentration Shift Keying (BCSK) that is proposed in [22]. From the viewpoint of the transmitter, no molecule is released to send 0 and certain number of molecules are released to send 1 for modulation. From the viewpoint of the receiver, the intended symbol is decoded as 1 if the concentration of the molecules is higher than certain threshold and as 0 if vice versa for demodulation.

While molecules can consistently move, the transmitter and the receiver are in the fixed topology with pre-defined radius. Although they all are assumed as spherical bodies, the relative sizes of molecules with respect to the fixed bodies are very low, but not negligible. For the sake of simplicity, we ignore the collisions between molecules. If molecules collide to the receiver, they are marked as received in the simulation. On the other hand, if they collide to the transmitter, they are bounced back. The displacement,  $\Delta X$ , of single molecule in one-dimensional environment in unit-time follows random distribution:

$$\Delta X \sim N(\mu, \sigma^2) = N(0, \sigma^2) \quad (1)$$

where  $\sigma = \sqrt{2D\Delta t}$ ,  $D$  is the diffusion coefficient and  $\Delta t$  is the step time. Note that the messenger molecules have inertia to stay in the same positions since  $\mu$  is equal to zero. The diffusion coefficient defines the inclination of the molecules to diffuse through the fluid. The higher the diffusion coefficient is, the faster the molecules move around. It can be easily calculated as follows:

$$D = \frac{K_b \cdot T}{b} \quad (2)$$

where  $K_b$  is the Boltzmann constant,  $T$  is the temperature in Kelvin and  $b$  is the friction coefficient between the molecules

and the fluid. The molecules propagate through the three-dimensional environment in our simulation and their total displacements,  $\vec{r}$ , are modelled as follows:

$$\vec{r} = (\Delta x, \Delta y, \Delta z) \quad (3)$$

which is computed by applying random displacements to three dimensions separately.

### B. Protrusion Model

We address one of the main limitations of communications via diffusion in this section. The limitation is that not every molecule is guaranteed to reach the receiver, which requires a large number of molecules to be released by the transmitter. This phenomena associates each molecule with probability of hit to the receiver,  $Prob_{hit}(d, t_s)$ , which is dependent to various factors including size of the receiver, distance between the transmitter and the receiver or environment itself. To mitigate the impacts of the limitation and increase the probability of hit, the paper [17] proposed the protrusion paradigm.

In this paper, each protrusion is modelled through single-link rigid cylindrical body stretching out from the receiver surface towards the transmitter. Each cylinder is defined by its radius  $r_{prot}$ , its length  $h_{prot}$  and three-dimensional position on the receiver surface. Just like the receiver does, when the protrusions capture the messenger molecules, they are received and then discarded from the simulation. The ways that the protrusion paradigm is expected to improve the probability of hit are two-fold. First, it implicitly reduces the distance between the transmitter and the receiver by directing the protrusions to the transmitter like antenna. Second, it increases the surface of area that can capture the messenger molecules to a great extent. That's why, it is stated in the paper [17] that having many thin protrusions instead of fewer thick ones is more advantageous.

## III. PROTRUSION LOCATION OPTIMIZATION PROBLEM

### A. Problem Definition

To the best of our knowledge, this is the premier work in the literature to propose the location optimization problem for the protrusions. The problem is modelled through constrained single-objective optimization problem in the paper. The location analysis of the receiver surface concerns with the optimal placement of the protrusions so that probability of hit of molecules is maximized. The problem has two different constraints to be satisfied: (1) the total number of the protrusions available for use must be limited and (2) the protrusions must stretch out from the receiver surface towards the transmitter.

In this section, we will provide the formal definition of the problem. Suppose a protrusion  $P_k \subseteq P$  is defined as five-dimensional tuple as  $P_k = \langle P_{kx}, P_{ky}, P_{kz}, P_{kr}, P_{kl} \rangle$  where  $\langle P_{kx}, P_{ky}, P_{kz} \rangle \subseteq \mathbb{R}^3$  denotes the position in three-dimensional space;  $\langle P_{kr} \rangle$  and  $\langle P_{kl} \rangle$  denote the radius and the length, respectively. On this basis, given protrusion set,

find a protrusion subset  $P$  so that the cumulative probabilities of hit of molecules is maximized:

$$F(P) = \max \sum_{m=1}^M Prob_{hit}^m(d, t_s) \quad (4)$$

where  $m$  represents the individual molecules,  $M$  represents the total number of molecules in the environment and  $F(P)$  is the objective function over protrusion subset. The first constraint in the problem is imposed by the following equation:

$$\sum_{k=1}^K \pi \cdot P_{kr}^2 \cdot P_{kl} = V_{prot} \quad (5)$$

where  $K$  represent the number of the protrusions in the environment and  $V_{prot}$  the maximum volumetric limit that can be occupied by the protrusions with respect to the receiver volume. Finally, the second constraint is imposed by the general equation for spheres with center  $(R_x, R_y, R_z)$  and radius  $R_r$ :

$$(P_{kx} - R_x)^2 + (P_{ky} - R_y)^2 + (P_{kz} - R_z)^2 = R_r^2 \quad (6)$$

$$P_{kx} \leq R_x, \forall P_k \subseteq P \quad (7)$$

The protrusion location optimization problem is *NP-Hard* to solve optimally. The time to solve the problem using current known algorithms rapidly grows with the size of total number of the protrusions. Therefore, the problem is addressed with the heuristic methods in the paper.

### B. Optimization Methods

As part of this paper, ten different algorithms for the protrusion location optimization problem are presented. Specifically, we can classify those algorithms into four different categories in terms of mechanisms they cope with the requirements of the problem as follows: (1) no protrusion methods, (2) distribution-based methods, (3) heatmap-based methods and (4) sequential selection methods. In this section, we briefly summarize their details.

1) *No-Protrusion Method (NOP)*: belongs to the first category where no protrusions are actively used to capture the molecules over the track. It is the baseline method to measure the performance of other methods using the protrusions.

2) *Random-Distributed Protrusion Method (RP)*: is a distribution-based method, in which the protrusions are spread over the surface of the receiver randomly. It is another baseline algorithm to understand whether using other more advanced algorithms to locate the protrusions are worth to further performance and efficiency.

3) *Uniformly-Distributed Protrusion Method (UP)*: is classified under distribution-based methods. It distributes the protrusions to the surface of the receiver uniformly. (see Algorithm 1)

---

**Algorithm 1 UP**


---

**Require:**  $P$  : Protrusion subset,  $p$  : Protrusion,  $K$  : Pre-defined number of protrusions

```

1:  $P = \emptyset$ 
2: while  $|P| \neq K$  do
3:    $p.y = \text{uniform}([-R_r, +R_r])$ 
4:    $p.z = \text{uniform}([-R_r, +R_r])$ 
5:    $p.x = R_r^2 - p.y^2 - p.z^2$ 
6:   if  $p.x \geq 0$  then
7:      $P = P + p^+$ 
8:   end if
9: end while
    
```

---

4) *Gaussian-Distributed Protrusion Method (GP)*: is a distribution-based method which spread the protrusions with respect to pre-specified Gaussian distribution,  $N(\mu, \sigma^2)$ . The main difference between *UP* and *GP* is that while the former one pays the same attention to all parts of the receiver surface, the latter one assigns more importance to the central regions of the receiver surface. (see Algorithm 2)

---

**Algorithm 2 GP**


---

**Require:**  $P$  : Protrusion subset,  $p$  : Protrusion,  $K$  : Pre-defined number of protrusions

```

1:  $P = \emptyset$ 
2: while  $|P| \neq K$  do
3:    $p.y = \text{normal}(\mu, \sigma^2, [-R_r, +R_r])$ 
4:    $p.z = \text{normal}(\mu, \sigma^2, [-R_r, +R_r])$ 
5:    $p.x = R_r^2 - p.y^2 - p.z^2$ 
6:   if  $p.x \geq 0$  then
7:      $P = P + p^+$ 
8:   end if
9: end while
    
```

---

5) *Heatmap-Distributed Protrusion Method (HP)*: belongs to the third category of optimization methods, which requires an extra step to locate the protrusions before the real experimentation, compared with the methods discussed so far. In this extra step, the messenger molecules are released into the environment and captured by the receiver. The heatmap is generated by counting the captured molecules to identify the best and worst regions of the surface. Then, unsupervised *K-means* clustering algorithm runs over the heatmap and locates the protrusions to the centroids.

6) *Sequential Forward Selection Protrusion Method (SFSP)*: is classified under sequential selection method. The sequential selection methods are originally proposed for feature/dimensionality reduction problem in order to minimize the classification error by reducing the curse-of-dimensionality effect. This method is adapted into the molecular communication domain, where we characterize the protrusions as individual features and select their subset. SFSP method starts from empty set, sequentially add the best protrusion that maximizes probability of hit when combined with already selected protrusions and terminates if pre-defined number of the protrusions is selected

7) *Sequential Backward Selection Protrusion Method (SBSP)*: is a sequential selection method that works in the opposite direction of *SFSP* method. *SBSP* starts from full set,

sequentially remove the worst protrusion with respect to probability of hit when combined with already selected protrusions and terminates if pre-defined number of the protrusions is selected. The main limitations of *SFSP* and *SBSP* methods are their inabilities to re-evaluate the protrusions after they are added and discarded, respectively.

8) *Plus-L Minus-R Selection Protrusion Method (LRSP)*: is another sequential selection method that aims to mitigate the impacts of the limitation of *SFS* and *SBS*. It starts from empty set, repeatedly adds  $L$  protrusions and then repeatedly discards  $R$  protrusions until the termination. On the other hand, *LRSP* suffers from theoretical difficulty to determine the optimal  $L$  and  $R$  values.

9) *Sequential Floating Forward Selection Protrusion Method (SFFSP)*: is the sequential selection method proposed to resolve the limitation of *LRS* method. *SFFSP* allows to infer the optimal  $L$  and  $R$  values from the protrusions themselves. It starts from empty set and after each forward step, it performs the backward step as long as the probability of hit increases until termination. The pseudo-code for *SFFSP* method is shown in Algorithm 3.

10) *Sequential Floating Backward Selection Protrusion Method (SFBSP)*: is the second sequential selection method proposed for the limitation of *LRS* method. *SFBSP* works in the opposite direction of *SFFSP*. This method starts from the full set and after each backward step, it performs the forward step as long as the probability of hit increases until termination. On the other hand, the drawbacks of those fourth category methods with respect to other category methods are that they require long computations to find the best positions for the protrusions and they may end up with sub-optimal solutions.

---

**Algorithm 3 SFFSP**


---

**Require:**  $P$  : Protrusion subset,  $p$  : Protrusion,  $K$  : Pre-defined number of protrusions,  $F$  : Objective function

```

1:  $P = \emptyset$ 
2: while  $|P| \neq K$  do
3:    $p^+ = \arg \max_{p \notin P} F(P + p)$ 
4:    $P = P + p^+$ 
5:    $p^- = \arg \max_{p \in P} F(P - p)$ 
6:   while  $F(P - p^-) > F(P)$  do
7:      $P = P - p^-$ 
8:   end while
9:    $p^- = \arg \max_{p \in P} F(P - p)$ 
10: end while
    
```

---

## IV. EXPERIMENTAL EVALUATION

## A. Experimental Setup

The simulator has been developed in Python for the given environment and propagation model. We evaluate the performance of ten algorithms in two different settings. In the first setting, we measure the effects of varying distances between the transmitter and the receiver up to four symbol durations. In the second setting, we measure the effects of varying number of the protrusions over varying distances. The performance evaluation is performed in terms of probability of hit. The

histogram of probability of hit throughout the experimental analysis is also shown in the paper.

The pre-experimental study shows that for *GP* method,  $N(0, 2)$  produces the best results to the given environments. Accordingly, for *LRSP* method, the forward and backward selection parameters,  $L$  and  $R$ , are equal to 6 and 1, respectively. The volume occupied by the protrusions,  $V_{prot}$  is equal to %5 of total receiver volume in the first setting while it may change correspondingly in the second setting. As recommended in [17], the receiver has many thin protrusions instead of fewer thick ones. Table 1. lists the default values for all other parameters used through the experiments.

TABLE I. SIMULATION PARAMETERS

Parameter	Value
$D$ (diffusion coefficient)	$79.4\mu m^2$
$r_{NeN}$ (receiver radius)	$10\mu m$
$r_{MM}$ (molecule radius)	$2.5nm$
$d$ (distance)	4, 8, 12, $16\mu m$
$t_s$ (symbol duration)	0.4, 1.6, 3.6, $6.4sec$
$\Delta t_s$ (time step)	$0.001sec$
$r_{prot}$ (protrusion radius)	$0.5\mu m$
$h_{prot}$ (protrusion length)	$3.5\mu m$

## B. Experimental Results

1) *Impacts of Varying Distance over Algorithms*: In the first experiment, we evaluate the effects of varying length between the transmitter and the receiver on the performance of algorithms. We expect gradual degradation in probability of hit of molecules to the receiver with increasing distance. The algorithms that yields robust results to changing distance are more preferred in this basis.

As seen in Table 2, the method that does not use the protrusions (*NOP*) at all produces the worst results by far in four consecutive symbol durations. The introduction of the protrusions into the receiver-side improves the performance to a great extent, as seen in the results of the randomly-distributed protrusion method (*RP*). However, it is very striking to realize that solely and randomly introducing the protrusions may not be sufficient to utilize their full capacities since uniformly-distributed (*UP*) and Gaussian-distributed (*GP*) outperform the *RP* method in all cases. Based on those results of *NOP* and *RP* baseline methods, it is shown that the location analysis of the protrusions on the receiver surface is worth to take into the consideration in the simulation modelling.

When comparing *UP* and *GP* methods, it can be deduced that while *GP* is considerably superior in shorter distances, *UP* is superior in longer distances. The probability of hit in *GP* in the first symbol duration, 0.995, which is the highest score that is achieved in our experiments and in the literature as well. The probability of hit has the highest significance in the first symbol durations and it becomes quite negligible after the second symbol durations but not zero. It means that the molecules that are released in the previous symbol duration can be received in the next symbol durations, which is called as *inter-symbol interference (ISI)*. *UP* and *GP* are the methods again that minimize *ISI* in the most of the cases. Note that

since *ISI* may happen after the first symbol duration, we do not consider it in the first symbol duration in the table.

The advantage of *GP* over *UP* in shorter distance is originated by the fact that the protrusions of *GP* is much closer to the release point of molecules than the protrusions of *UP*. However, this advantage gradually fades away with increasing distance due to diffusion dynamics in the fluid and uniform distribution of the protrusions become more favourable. Although the results of heatmap-based and sequential feature selection-based methods are promising, they are not superior in any single case. From this perspective, it may not be good to use sequential feature selection-based methods by considering their extra long temporal computational requirements.

2) *Impacts of Varying Number of Protrusions over Algorithms*: In the second experiment, we evaluate the effects of varying number of the protrusions on the receiver surface. We look for the cut-off point in the plateau where no extra protrusion can improve the performance further. This experiment is important to understand what the optimal number of the protrusions is in accordance with the varying distance and how much resource for the protrusions are wasted by using  $V_{prot}$  as %5. Since advantage of having the protrusions is gradually decreasing with increasing distance, we expect to reach cut-off point earlier in longer channels. For this experiment, only two baseline algorithms, *NOP* and *RP*, and two best algorithms, *UP* and *GP*, are considered.

The results can be seen in terms of probability of hit in Fig. 3. where  $x$ -axis denote the number of the protrusions and  $y$ -axis denotes the performance indicator for the first symbol duration. It can be inferred that when distance is  $4\mu m$  and number of the protrusions is 10, the performance of *GP* suddenly increases from %65 to %93. On the other hand, *UP* needs 20 protrusions to reach that performance level. We see that even their performance improve with increasing number of the protrusions, they end up with the same plateau after it is 40.

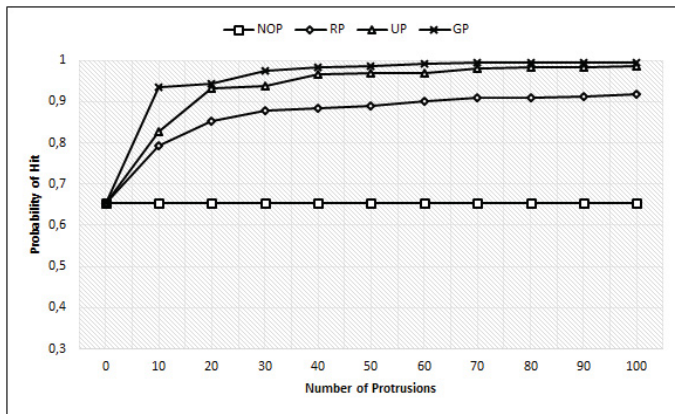
The effects of increasing distance between the transmitter and the receiver on the optimal number of the protrusions are seen in Fig 3. The first observation is that the slope of performance until plateau has decreasing trend with respect to increasing distance. Moreover, the algorithms reach plateau earlier with increasing distance as well. When distance is  $16\mu m$ , the advantage of the protrusions is gone to a great extent. If we fix the percentage-based incremental gain of the protrusions as %23 for *GP*, we find that it is reached by using 100 protrusions in  $16\mu m$ , 50 protrusions in  $12\mu m$ , 20 protrusions in  $8\mu m$  and finally 10 protrusions in  $4\mu m$ .

3) *Analysis of Probability of Hit by Histograms*: In this part, we qualitatively evaluate the effects of the receiver surface and the protrusions on capturing the molecules in the fluid. Our goal is to characterize hot spots on the surface and the protrusions; and relations between those hot spots and varying distance between the transmitter and the receiver. The histograms are provided in Fig. 4 for *NOP*, *RP*, *UP* and *GP* for  $d = 4, 8, 12, 16\mu m$ . For each algorithm and each distance in the Fig. 4, the first snapshot is the front view of the receiver

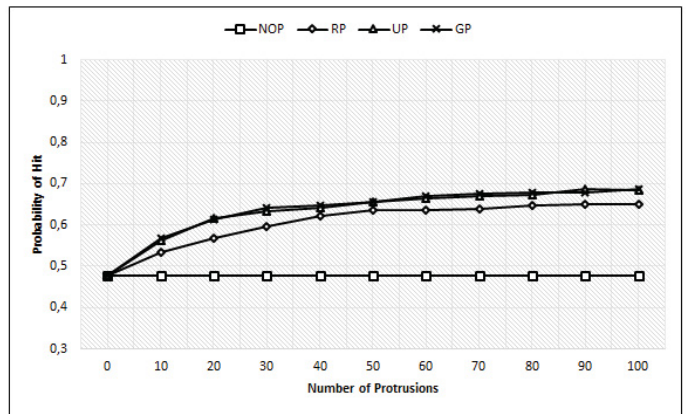
TABLE II. IMPACTS OF VARYING CHANNEL DISTANCE OVER ALGORITHMS

		$d = 4\mu m$									
		NOP	RP	UP	GP	HP	SFSP	SBSP	LRSP	SFFSP	SFBSP
$0 - 1t_s$		0.6541	0.9103	0.9794	<b>0.995</b>	0.9938	0.9854	0.9846	0.9839	0.9849	0.9817
$1 - 2t_s$		0.7218	0.9254	0.982	<b>0.9953</b> †	0.9946	0.9876	0.9869	0.9851	0.988	0.9838
$2 - 3t_s$		0.745	0.9312	0.9839	<b>0.9956</b> †	0.9951	0.9881	0.9884	0.9868	0.9889	0.9857
$3 - 4t_s$		0.7595	0.935	0.9845	<b>0.9957</b> †	0.9953	0.9885	0.9888	0.9871	0.9896	0.9865
		$d = 8\mu m$									
		NOP	RP	UP	GP	HP	SFSP	SBSP	LRSP	SFFSP	SFBSP
$0 - 1t_s$		0.4807	0.6463	0.6737	<b>0.679</b>	0.6746	0.6748	0.6743	0.6748	0.6739	0.6706
$1 - 2t_s$		0.5388	0.681	0.7102	<b>0.7117</b> †	0.7083	0.7111	0.7075	0.7097	0.7101	0.7054
$2 - 3t_s$		0.563	0.696	0.7229	<b>0.7244</b>	0.722	0.721†	0.7216	0.7211	0.7221	0.7203
$3 - 4t_s$		0.5763	0.7055	0.7301	<b>0.7309</b> †	0.7292	0.7296	0.7305	0.7279	0.7297	0.7285
		$d = 12\mu m$									
		NOP	RP	UP	GP	HP	SFSP	SBSP	LRSP	SFFSP	SFBSP
$0 - 1t_s$		0.3664	0.4608	<b>0.4902</b>	0.4673	0.4848	0.4806	0.4838	0.485	0.4812	0.4789
$1 - 2t_s$		0.4112	0.4993	<b>0.5275</b> †	0.5063	0.5222	0.5201	0.5218	0.5244	0.5194	0.5197
$2 - 3t_s$		0.431	0.5138	<b>0.5442</b>	0.5222	0.5398	0.5369	0.5368	0.5384†	0.5341	0.5374
$3 - 4t_s$		0.4224	0.5245	<b>0.5537</b> †	0.5336	0.5504	0.5473	0.5472	0.5482	0.5439	0.5478
		$d = 16\mu m$									
		NOP	RP	UP	GP	HP	SFSP	SBSP	LRSP	SFFSP	SFBSP
$0 - 1t_s$		0.3055	0.3643	<b>0.3859</b>	0.3649	0.3757	0.3739	0.3791	0.3731	0.3747	0.3799
$1 - 2t_s$		0.3408	0.4015	<b>0.4194</b> †	0.3998	0.4147	0.4113	0.4131	0.4111	0.4111	0.4136
$2 - 3t_s$		0.3572	0.4172	<b>0.4335</b> †	0.4166	0.4313	0.4274	0.4284	0.4277	0.4267	0.429
$3 - 4t_s$		0.3683	0.4269	<b>0.4423</b> †	0.4262	0.4417	0.437	0.438	0.4386	0.4367	0.4383

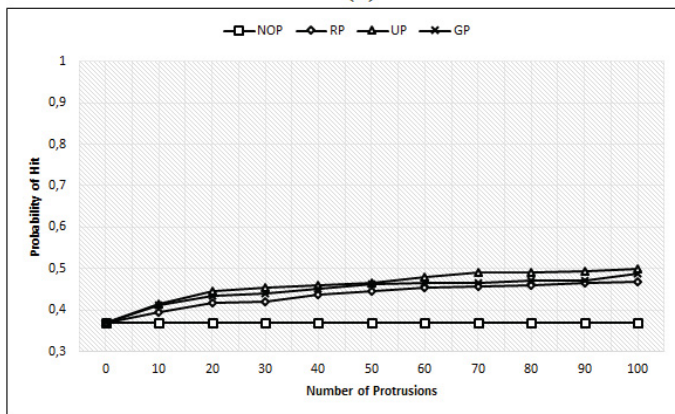
† denotes the minimum inter-symbol interference (ISI).



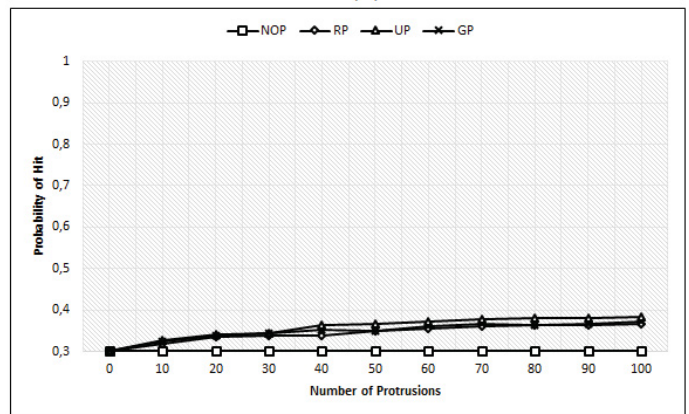
(a)



(b)



(c)



(d)

Fig. 3. Probability of hit over varying number of the protrusions for  $NOP$ ,  $RP$ ,  $UP$  and  $GP$ : (a) for  $d = 4\mu m$ , (b) for  $d = 8\mu m$ , (c) for  $d = 12\mu m$ , (d) for  $d = 16\mu m$

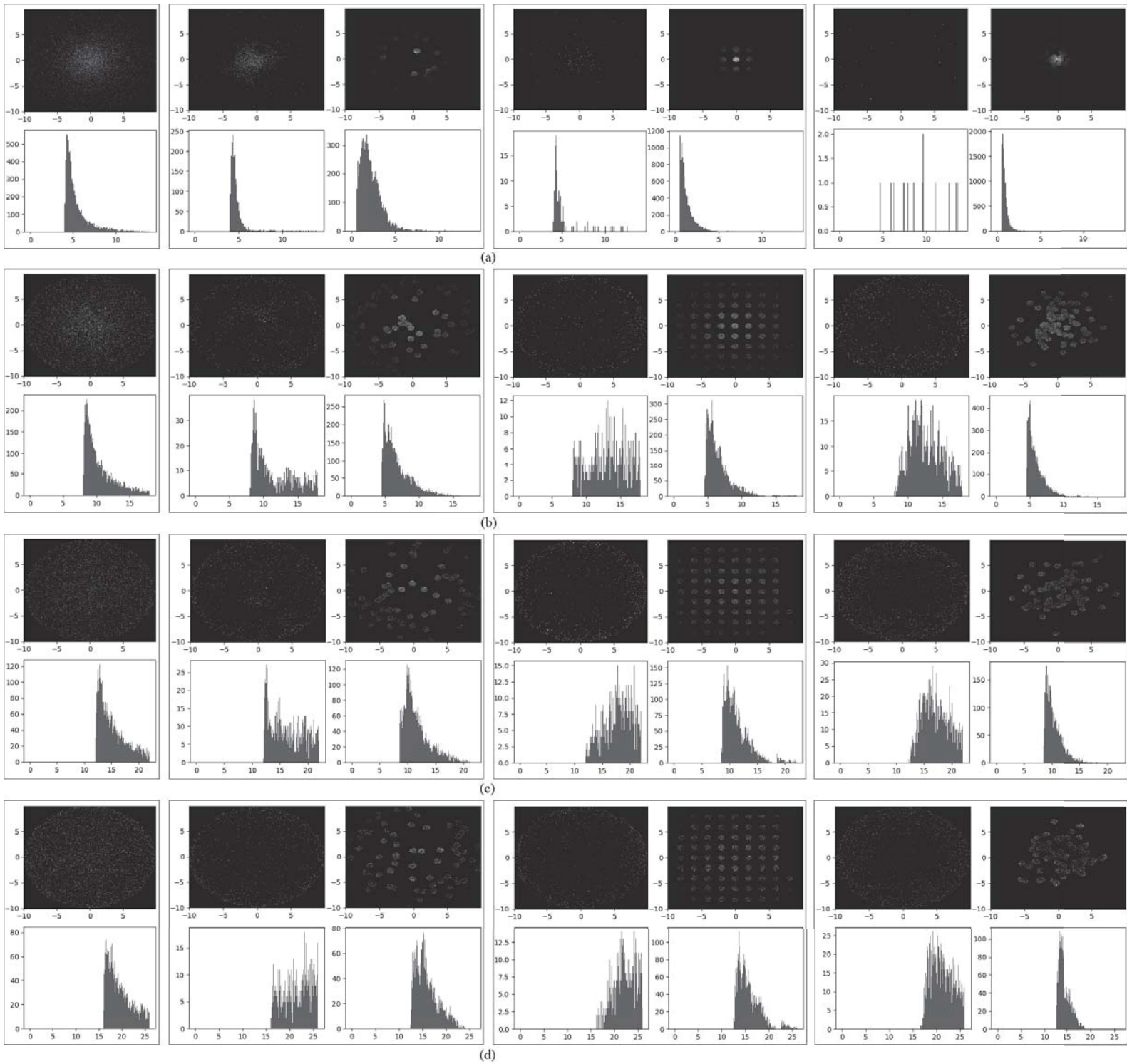


Fig. 4. Snapshots and histograms of molecules hit to the receiver and the protrusions for *NOP*, *RP*, *UP* and *GP*, respectively: (a) for  $d = 4\mu\text{m}$ , (b) for  $d = 8\mu\text{m}$ , (c) for  $d = 12\mu\text{m}$ , (d) for  $d = 16\mu\text{m}$ .

and the corresponding histogram with respect to distance is underneath it; the second snapshot is the front view of the protrusions and the corresponding histogram with respect to distance is underneath it as well. The more collisions occur at a spot, the brighter that spot is. Note that no snapshot of the protrusions and corresponding histogram are shown for *NOP*.

On this basis, it is observed for  $d = 4\mu\text{m}$  that when no protrusion is available, all the molecules are captured by the receiver itself and hot spot is the central region. If we look at its histogram, the surface towards the release point has the highest number of molecules. However, when the protrusions are available, large portions of the molecules are captured by them. As seen in the snapshots for *UP* and *GP*, their central regions are brighter than the others, which means that very high number of molecules are captured. This can be validated by looking at their corresponding histograms. These results are also consistent with the the results of the first experiment.

It is certain that regions towards the release points are the hot spots nearly in all cases. Besides, the number of molecules captured by the protrusions exponentially decreases with respect to distance. Two factors play roles there. First, since more number of molecules are captured at outer parts of the protrusions, very small portions of molecules left behind for inner parts of the protrusions. Second, the virtually-created area of the protrusions exponentially decrease towards the center of the receiver and it is assumed as zero at the surface where all molecules reaching there are considered as captured. With increasing distance, we can observe that importance of central regions of both the receiver and the protrusions gradually fades away and all regions becomes equally important since the brightness of the protrusions are now uniformly distributed. If this is the case, the superiority of *UP* is not surprising any more at all.

## V. CONCLUSION

Although molecular communication lives its infancy, it is very promising concept in nanonetworking. There still exist numerous issues to be resolved, one of which is the reception enhancement of the protrusions. To address that issue, we propose the protrusion location optimization problem in this paper. In order to enhance the reception capabilities of the protrusions for better communication between the transmitter and the receiver, ten different algorithms are presented according to the requirements of the problem.

We perform experimental evaluation and analyse their performance in two different settings. The experiments are consistent with the existing works in the literature. Based on our evaluations, we find that Gaussian-distributed protrusions yield better performance in shorter channels while uniformly-distributed protrusions is superior in longer channels. The feature-based algorithms seem as not preferable for this problem due to worse results and long computational complexity. For the future work, we are planning to model the protrusions as multi-joint links instead of single straight structure and propose a novel metric to measure the structural goodness of the protrusions.

## REFERENCES

- [1] I.F. Akyildiz, F. Brunetti, "C. Blazquez, Nanonetworks: A new communication paradigm," *Computer Networks*, vol. 52, no. 12, pp. 2260-2279, 2008.
- [2] B. Atakan, O. B. Akan, "Body area nano-networks with molecular communications in nanomedicine," *IEEE Communications Magazine*, pp. 28-34, 2012.
- [3] U. A. K. Chude-Onkonkwo, R. Malekian, B. T. Maharaj and A. V. Vasilakos, "Molecular communication and nanonetwork for targeted drug delivery: a survey," *IEEE Communications Surveys & Tutorials*, vol. 19, no. 4, pp. 3046-3096, 2017.
- [4] F. Afsana, M. Asif-Ur-Rahman, M. R. Ahmed, M. Mahmud and M. S. Kaiser, "An energy conserving routing scheme for wireless body sensor nanonetwork communication," *IEEE Access*, vol. 6, pp. 9186-9200, 2018.
- [5] F. Gulec, B. Atakan, "Distance estimation methods for a practical macroscale molecular communication system," *Nano Communication Networks*, vol. 24 (100300), 2020.
- [6] A. Enomoto, M. Moore, T. Nakano, R. Egashira, T. Suda, "A molecular communication system using a network of cytoskeletal filaments," *9th Nanotechnology Conference (NANOTECH)*, pp. 725-728, 2006.
- [7] T. Suda, M. Moore, T. Nakano, R. Egashira, A. Enomoto, "Exploratory research on molecular communication between nanomachines," *Genetic and Evolutionary Computation Conference (GECCO'05)*, 2005.
- [8] T. Nakano, T. Suda, M. Moore, R. Egashira, A. Enomoto, K. Arima, "Molecular communication for nanomachines using intercellular calcium signaling," *5th IEEE Conference on Nanotechnology (IEEE-NANO'05)*, vol. 2, pp. 478-481, 2005.
- [9] L. P. Gin'e, I. F. Akyildiz, "Molecular communication options for long range nanonetworks," *Computer Networks*, vol. 53, no. 16, pp. 2753-2766, 2009.
- [10] N. Farsad, H. B. Yilmaz, A. Eckford, C. Chae and W. Guo, "A comprehensive survey of recent advancements in molecular communication," *IEEE Communications Surveys & Tutorials*, vol. 18, no. 3, pp. 1887-1919, 2016.
- [11] P. Yeh, K. Chen, Y. Lee, L. Meng, P. Shih, P. Ko, et al., "A new frontier of wireless communication theory: diffusion-based molecular communications," *IEEE Wireless Communications*, vol. 19, no. 5, pp. 28-35, 2012.
- [12] M. S. Kuran, H. B. Yilmaz, T. Tugcu and B. Ozerman, "Energy model for communication via diffusion in nanonetworks," *Nano Communication Networks*, vol. 1, no. 2, pp. 86-95, 2010.
- [13] M. S. Kuran, H. B. Yilmaz, T. Tugcu and I. F. Akyildiz, "Interference effects on modulation techniques in diffusion based nanonetworks," *Nano Communication Networks*, vol. 3, no. 1, pp. 65-73, 2012.
- [14] T. Nakano, Y. Okaie, S. Kobayashi, T. Hara, Y. Hiraoka and T. Haraguchi, "Methods and Applications of Mobile Molecular Communication," *Proceedings of the IEEE*, vol. 107, no. 7, pp. 1442-1456, 2019.
- [15] P. T. Caswell, T. Zech, "Actin-Based cell protrusion in a 3D matrix," *Trends in Cell Biology*, vol. 28, no. 10, pp. 823-834, 2018.
- [16] P. A. Gagliardi, A. Puliafito, L. di Blasio, F. Chianale, D. Somale, G. Seano, et al., "Real-time monitoring of cell protrusion dynamics by impedance responses," *Nature Scientific Reports*, vol. 5, no. 10206, 2015.
- [17] G. Genc, H. B. Yilmaz, T. Tugcu, "Reception enhancement with protrusions in communication via diffusion," *First International Black Sea Conference on Communications and Networking (BlackSeaCom)*, pp. 89-93, 2013.
- [18] C. Boonmee, M. Arimura, T. Asada, "Facility location optimization model for emergency humanitarian logistics," *International Journal of Disaster Risk Reduction*, vol. 24, pp. 485-498, 2017.
- [19] J. Yao, X. Zhang, A. T. Murray, "Location optimization of urban fire stations: Access and service coverage," *Computers, Environment and Urban Systems*, vol. 73, pp. 184-190, 2019.
- [20] X. Fan, X. Wen, S. Jiang, "Research on path planning and location optimization of quantum wireless sensor networks," *Journal of Computers*, vol. 31, no. 5, pp. 324-330, 2020.
- [21] J. Brimberg, "The Fermat-Weber location problem revisited," *Mathematical Programming*, vol. 71, pp. 71-76, 1995.
- [22] M. S. Kuran, H. B. Yilmaz, T. Tugcu and I. F. Akyildiz, "Modulation techniques for communication via diffusion in nanonetworks," *IEEE International Conference on Communications (ICC)*, pp. 1-5, 2011.